

PCCP

Accepted Manuscript



This is an *Accepted Manuscript*, which has been through the Royal Society of Chemistry peer review process and has been accepted for publication.

Accepted Manuscripts are published online shortly after acceptance, before technical editing, formatting and proof reading. Using this free service, authors can make their results available to the community, in citable form, before we publish the edited article. We will replace this *Accepted Manuscript* with the edited and formatted *Advance Article* as soon as it is available.

You can find more information about *Accepted Manuscripts* in the [Information for Authors](#).

Please note that technical editing may introduce minor changes to the text and/or graphics, which may alter content. The journal's standard [Terms & Conditions](#) and the [Ethical guidelines](#) still apply. In no event shall the Royal Society of Chemistry be held responsible for any errors or omissions in this *Accepted Manuscript* or any consequences arising from the use of any information it contains.

Fragmentation Mechanism of the Generation of Colloidal Copper(I) Iodide Nanoparticles by Pulsed Laser Irradiation in Liquids

Christian Alexander Schaumberg,^a Markus Wollgarten,^b and Klaus Rademann^{a*}

Received Xth XXXXXXXXXXXX 20XX, Accepted Xth XXXXXXXXXXXX 20XX

First published on the web Xth XXXXXXXXXXXX 200X

DOI: 10.1039/b000000x

Pulsed laser ablation in liquids (PLAL) is a versatile route to stable colloids without the need for stabilizing agents. The use of suspensions instead of bulk targets further simplifies the experimental set-up and even improves the productivity. However, the utilization of this approach is hindered by limited knowledge about the underlying mechanisms of the nanoparticle formation. We present the synthesis of copper(I) iodide nanoparticles via ns-pulsed laser irradiation of CuI powder suspended in water or ethyl acetate. A thorough study of the nanoparticle size by transmission electron microscopy reveals a log-normal distribution with a mean diameter of 31 nm (± 11 nm) in water and 18 nm (± 7 nm) in ethyl acetate. The duration of the laser irradiation appears to have only a minor influence on the size distribution. Selected area diffraction and electron energy-loss spectroscopy verify the chemical composition of the generated CuI nanoparticles. While comparable precursors like CuO and Cu₃N follow a reductive ablation mechanism, a fragmentation mechanism is found for CuI. With a productivity of 1.7 $\mu\text{g}/\text{J}$ this pulsed laser fragmentation in liquids (PLFL) proves to be an efficient route to colloidal CuI nanoparticles.

1 Introduction

Laser ablation of solids is a well known method for the generation of clusters and small particles.¹ A major development in this field was the pulsed laser ablation in liquids (PLAL). Here, the ablation target is immersed in a liquid.² The step from a low pressure environment to the liquid comes with several changes in the ablation process. As the laser initiated plasma is formed, the liquid confines its expansion. This results in a higher pressure and temperature inside the plasma and even in the formation of shock waves.^{3,4} This is seen as the reason for the higher ablation efficiency of PLAL compared to ablation in air or vacuum. As the hot plasma is in direct contact with the surrounding liquid, chemical reactions can occur at the interface. This may give access to the synthesis of new materials.⁵ The generated particles are often covered by a carbon layer which originates from the decomposition of the organic immersion liquid.⁶ In many cases, this results in an undesirable blocking of the particle surface. But in other cases, it may improve the colloidal stability or even enhance the catalytic activity.⁷ After each laser pulse, the surrounding liquid results a fast cooling of the ablated material, giving access to metastable materials.⁸ The most important consequence of performing the ablation in a liquid is the for-

mation of stable colloids. As colloids can be handled like chemical solutions, handling is safe and convenient.

Colloidal solutions may also be synthesized by various other methods. However, most of these rely on additional stabilizing agents.⁹ Thus, for applications where additives are not tolerable, PLAL is the superior alternative.^{10,11}

In addition to the ablation of solid targets, the use of powders suspended in a liquid is also possible. It further simplifies the experimental set-up and even leads to new materials. The nanoparticle generation by laser irradiation of a suspended powder can lead to higher productivity, which becomes useful if higher laser powers are not available or desirable. The first report on this approach describes the laser irradiation of a copper(II) oxide powder suspended in 2-propanol.¹² Interestingly, the irradiation of CuO results in the formation of metallic copper nanoparticles. Recently, it has been shown that this reductive ablation process appears to be a general phenomenon, as it is observed for several copper containing precursors.¹³ In the first step a plasma is formed at the μm -sized precursor powder and thereby the copper atoms are ablated. The copper atoms and ions nucleate and form small primary particles with a diameter between 1 and 5 nm. In a second step these primary particles coalesce to larger nanoparticles with a diameter of about 20 nm. This two step process leads to a bimodal size distribution. Besides this reductive ablation process there is a second possible route to obtain nanoparticles from μm -sized powders. Here, the precursor powder is fragmented by the laser light under preservation of chemical composition. In distinction to PLAL the latter mechanism can be classified as

^a Department of Chemistry, Humboldt-Universität zu Berlin, Brook-Taylor-Straße 2, 12489 Berlin, Germany. E-mail: klaus.rademann@chemie.hu-berlin.de

^b Helmholtz-Zentrum Berlin für Materialien und Energie GmbH, Hahn-Meitner-Platz 1, 14109 Berlin, Germany.

pulsed laser fragmentation in liquids (PLFL). In order to gain insights into the characteristics of the involved processes, our work is focussed on the PLFL of μm -sized copper(I) iodide powder suspended in ethyl acetate.

Besides the mentioned mechanistic considerations, a simple route to synthesize CuI nanoparticles is of general interest because of the large exciton binding energy of CuI.¹⁴ In addition, the formation of stable CuI colloids by PLFL is an easy way to evenly distribute CuI in solvents where the solubility of CuI is low. This may be useful for copper catalysed organic reactions.^{15,16}

2 Experimental Section

Copper(I) iodide (99%, Riedel-de Haën, Germany) and ethyl acetate (99.5%, Roth, Germany) were used without further purification. An environmental scanning electron microscope (ESEM) TM-1000 (Hitachi, Japan) equipped with a back scattered electron detector and set to an accelerating voltage of 15 kV was used to determine the particles size distribution of the CuI powder.

The pulsed laser fragmentation was performed with a q-switched Nd:YAG laser Ultra (Quantel, France). The 2nd harmonic (532 nm, 45 mJ/pulse, 6 ns) was used without further focusing the beam. The resulting beam had a diameter of approximately 3 mm and a laser fluence of up to 0.64 J/cm².

19 mg CuI powder (0.1 mmol) was suspended in 7.8 mL ethyl acetate or deionised water and vigorously stirred during the laser irradiation. The used polypropylene vessels were completely filled with the suspension and closed by pressing a glass slide to the opening. Care was taken that no gas bubbles remained in the reaction vessel. The laser beam entered the suspension from the top through the glass slide. The irradiation was performed with 20 Hz for treatment times from 20 s up to 10 min resulting in 400 to 12000 laser pulses. In order to separate the resulting colloid from the precursor powder, the suspension was allowed to sediment for 1 h. Alternatively, the suspension was centrifuged for 5 min with a moderate speed of 2500 rpm.

Transmission electron microscopy (TEM), energy-filtered transmission electron microscopy (EFTEM), and electron energy-loss spectroscopy was performed with a Libra 200FE TEM (Zeiss, Germany) equipped with an Omega-type energy filter and an Ultrascan CCD camera (Gatan, U.S.A.). The accelerating voltage was set to 200 kV. 20 μL of the colloid were dropped onto carbon-coated copper grids (CF200-Cu, Electron Microscopy Sciences, U.S.A.) or silicon nitride membranes (DuraSiN, Electron Microscopy Sciences, U.S.A.). An energy-selecting slit was used to exclude electrons which suffered inelastic scattering. This zero loss energy filtering was applied to improve the image contrast of the TEM images.

In order to improve the accuracy of the lattice constant measurements, the electron diffraction patterns were calibrated using an Au standard sputtered onto each TEM grid.

EFTEM images were taken with an automated routine providing spatial drift correction.¹⁷ The width of the energy selecting slit was set to 20 eV. For the iodine map the M_{4,5} edge at 631 eV was used and 3 pre-edge images were recorded. In order to reach a signal to noise ratio greater than 6, 20 images were taken and averaged for each energy.

EELS data were collected with a four-fold hardware binning and with a filter entrance aperture equivalent to a sample area with a diameter of 125 nm. In order to improve the signal-to-noise ratio and avoid artefacts, up to 100 spectra were accumulated at different areas of the CCD. The EEL spectra were background-corrected by subtraction of a power law function fitted to the pre-edge region. In addition, the core edge spectra were deconvolved with the corresponding low loss spectra with the GSM 1.8 software (Gatan, U.S.A.).

Flame atomic absorption spectrometry was used to determine the yield and the productivity of the PLFL of the CuI suspensions. An aliquot of the colloid was heated until the ethyl acetate was completely evaporated. Subsequently, the sample was dissolved in concentrated nitric acid at elevated temperatures and diluted with deionized water. The copper content was measured with an AAnalyst 200 (PerkinElmer, U.S.A.).

In order to determine the particle size distributions, the diameter of at least 700 individual particles were measured with the ImageJ 1.48k software (National Institutes of Health, U.S.A.). The minor axis was measured in case of non-spherical particles. The data was fitted to a cumulative log-normal distribution: $F(d; \mu, \sigma) = 0.5(1 + \text{erf}((\ln(d) - \mu)/(\sigma\sqrt{2})))$. The adjusted coefficient of determination (\bar{R}^2) was at least 0.99 for each fit. In the present paper, the “size” of the particles always refers to the mean value of the diameter $\langle d \rangle = e^{\mu + \sigma^2/2}$ gained from the log-normal fits, while the values in the brackets represent the corresponding standard deviations $s = \langle d \rangle (e^{\sigma^2} - 1)^{1/2}$. The plotted size distributions are the normalized probability density functions of the fits.

The analytical disc centrifuge measurements were performed at 20000 rpm with a DC24000 disc centrifuge (CPS Instruments, U.S.A.).

3 Results and Discussion

Pulsed laser fragmentation in liquids (PLFL) of copper(I) iodide powder in water or ethyl acetate reduces the particle size by about three orders of magnitude. Thus, nanoparticles are generated from μm -sized precursor particles.

Fig. 1a shows an ESEM image of the precursor powder. The size of these particles is $\langle d \rangle = 16.8 \mu\text{m}$ ($s = 5.2 \mu\text{m}$). Af-

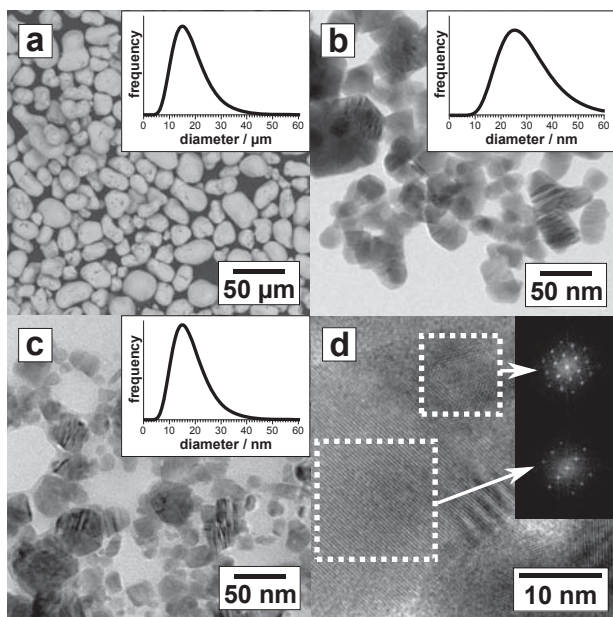


Fig. 1 PLFL of Copper(I) iodide (a) ESEM image of the CuI precursor powder (b) TEM image of CuI nanoparticles generated in water, (c) TEM image of the CuI nanoparticles generated in ethyl acetate, (d) HR-TEM image with FFT images of the depicted areas.

ter 12000 laser pulses in water the resulting irregular shaped nanoparticles have a size of $\langle d \rangle = 30.9$ nm ($s = 11.0$ nm) as shown by TEM (Fig. 1b). Particles generated in ethyl acetate have a size of $\langle d \rangle = 18.4$ nm ($s = 7.0$ nm) (Fig. 1c). The synthesized nanoparticles are crystalline as it can be seen in the high resolution TEM image (Fig. 1d). Particles are single- as well as polycrystalline. This holds true for the fragmentation in water, as well as in ethyl acetate.

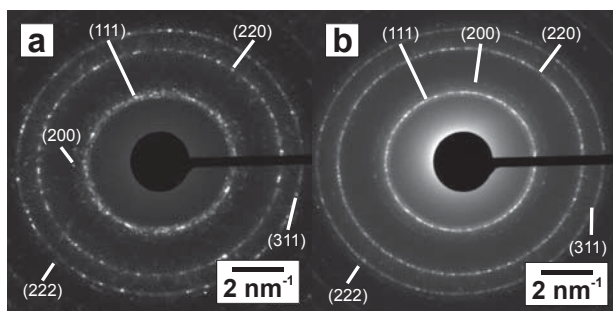


Fig. 2 Selected area diffraction images showing the sphalerite crystal structure of copper(I) iodide nanoparticles generated (a) in water, (b) in ethyl acetate.

Indexing of the diffraction pattern (Fig. 2a and 2b) indicates a face centred cubic structure. The lattice constant has been measured to be 0.60 nm (± 0.01 nm), which is

reasonable close to the value for CuI given in the literature (0.60545 nm).¹⁸ Despite some differences due to different crystallite sizes, the diffraction pattern of the particles generated in water and ethyl acetate are identical. Apparently the choice of the liquid has a major impact on the nanoparticle size, but not on the chemical composition or crystal structure.

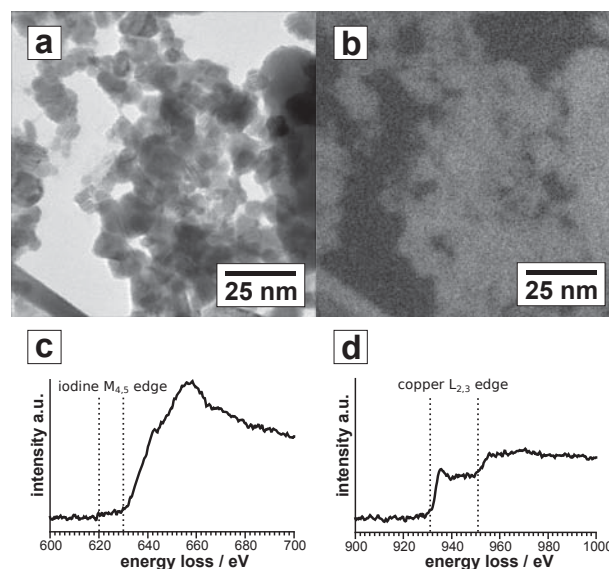


Fig. 3 Copper(I) iodide nanoparticles synthesized via PLFL in ethyl acetate (a) TEM image used for drift correction during EFTEM measurements, (b) iodine distribution map, (c) EELS at the iodine $M_{4,5}$ edge, (d) EELS at the copper $L_{2,3}$ edge. The dotted lines mark the edge onset for the respective elements.¹⁹

In Fig. 3a a bright field TEM image of the nanoparticles is shown. Fig. 3b depicts the same area but this time the iodine map measured at the $M_{4,5}$ edge. The bright areas in this iodine distribution map coincide with the particle positions in the bright field TEM image. Thus, the iodine is evenly distributed in all nanoparticles. The EELS measurements at the iodine $M_{4,5}$ edge (Fig. 3c) and at the copper $L_{2,3}$ edge (Fig. 3d) prove the presence of both elements. Besides minor carbon contamination, no signal from other elements is present in the EELS data. This is an important finding as the laser ablation or fragmentation of copper containing materials under atmospheric conditions often leads to the formation of Cu_2O or CuO . The formation of copper oxides can be excluded, as the characteristic white lines at the copper $L_{2,3}$ edge are missing.

The diffraction patterns in combination with the EFTEM and EELS investigation unambiguously prove that all generated nanoparticles consist of crystalline copper(I) iodide. This is a crucial difference compared to the irradiation of other copper compounds like CuO , Cu_3N , $Cu(N_3)_2$ and Cu_2C_2 where

the laser irradiation always leads to metallic copper nanoparticles.¹³ This suggests that the formation of the CuI particles does not follow the ablation, nucleation, and coalescence mechanism found for the other copper precursors.

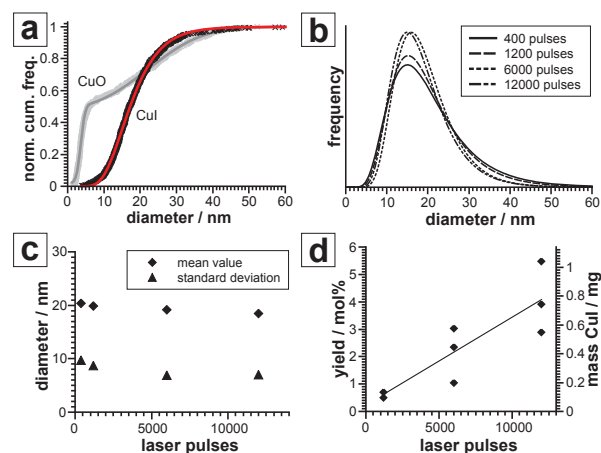


Fig. 4 Size distribution and yield of the PLFL of CuI in dependence of the duration of the irradiation: (a) normalized cumulative frequency of a representative sample after 12000 laser pulses with 1029 individual nanoparticles being evaluated, (b) normalized, estimated density functions of the diameter of the nanoparticles, (c) mean value and standard deviation of the size distributions, (d) yield and absolute mass of the generated nanoparticles.

A key feature to understand the mechanism of the nanoparticle generation by laser irradiation is a thorough evaluation of the size distribution. The ablation of CuO, Cu₃N, Cu(N₃)₂ and Cu₂C₂ precursors results in a bimodal Gaussian like size distribution. During the irradiation, the portion of larger particles increases, pointing to a coalescence mechanism.¹³ In the case of CuI, the size of the nanoparticles follows a log-normal distribution. Fig. 4a exemplarily shows the cumulative frequency of the size of the CuI nanoparticles generated in ethyl acetate and the log-normal fit. It is clear that this behaviour is exceptional when compared to the data of the laser irradiation of CuO in the same solvent (shown in light grey). The size distribution for samples with varying irradiation durations are depicted in Fig. 4b. At first glance, the size distributions for 400 to 12000 pulses are similar. However, with longer irradiation times the distribution becomes narrower, shifting the mean value to lower values, while the position of the maximum does not change. This is also visible in Fig. 4c, where the mean value and the standard deviation are plotted over the number of pulses. The decrease of the mean value and the standard deviation with ongoing irradiation is evident, but the dependence on the number of pulses is weaker than expected. This leads to several important conclusions. (a) There is no laser driven particle growth as it was observed for the irra-

diation of CuO, Cu₃N, Cu(N₃)₂ and Cu₂C₂ precursors. (b) There is a stable final size of the particles. (c) This final size is reached after less than 400 pulses.

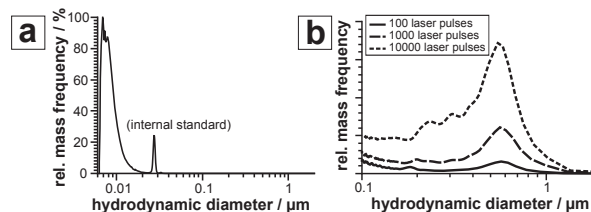


Fig. 5 Hydrodynamic diameter determined by analytical disc centrifugation: (a) size distribution after 100 pulses, (b) comparison of the 100 nm < d < 2 μm size fraction after 100, 1000, and 10000 laser pulses.

In order to gain a more general overview over the size distribution, the synthesized colloids were investigated via analytical disc centrifugation. Figure 5a shows that nanoparticles with hydrodynamic diameters of 20 nm and below are the predominant product of the laser irradiation of CuI. The mean hydrodynamic diameter of the particles differs slightly from the mean diameter obtained by TEM. This is likely to be caused by the non-sphericity of the particles. When taking a closer look, a second fraction of particles can be found with diameters of about 600 nm. This fraction grows as more laser pulses are applied as shown in Figure 5b. These particles are the reason that the colloid becomes turbid during the laser irradiation. However, when the results of the analytical disc centrifuge are evaluated quantitatively it becomes clear, that the particles with diameters ranging from 200 nm to 2 μm only account for less than 1 % of the total mass of CuI in the colloid.

Taking into account that (a) the chemical composition does not change, (b) only few particles smaller than 5 nm are generated, and (c) particle coalescence is not observed, it can be stated that the formation of the CuI nanoparticles is based on a fragmentation rather than an ablation mechanism. Therefore, the generation of CuI nanoparticles from μm-sized CuI powder can be characterized as PLFL rather as PLAL. Fig. 6 gives an overview of both mechanisms. In principle both mechanisms should be possible at the same time. However, for the generated nanoparticles only one or the other mechanism is observed for a certain precursor. It is not clear why CuI favours the fragmentation mechanism. Obviously, CuI does not absorb enough energy during a laser pulse to make an evaporation of copper and iodine atoms possible in a larger extend. Thus, no copper or copper oxide particles are observed, in contrast to precursors like CuO or Cu₃N. But sufficient energy is absorbed to introduce stress to the crystal resulting in a fragmentation. It is likely that the formation of

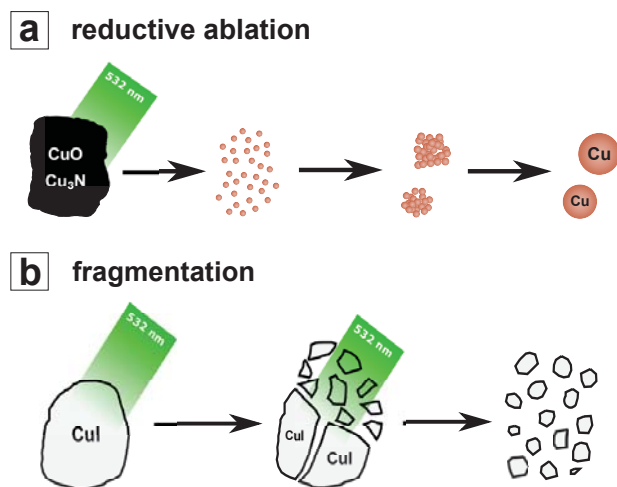


Fig. 6 Schematic of the mechanism of (a) the reductive ablation of CuO or Cu₃N and (b) the fragmentation of CuI.

shock waves play a major role as has been discussed in literature.^{20–22} This fragmentation mechanism is consistent with investigations on ZnO and B₄C.²³ Further hints on this conclusion can be gained from samples with less than 100 laser pulses. However, this becomes quite challenging, as the small amount of generated particles will drastically reduce the statistical significance of the measured size distributions.

The issue of sufficiently high productivity is not only important for investigating the mechanism, but is also of great interest for practical applications of this synthetic route. Fig. 4d shows the dependence of the fragmentation yield on the number of laser pulses after separating remaining precursor powder and larger fragments by centrifugation. Thus the yield represents the fraction of the precursor material processed to particles smaller than roughly 100 nm. From this data, the productivity in ethyl acetate averages to 1.7 μg/J (± 0.6 μg/J). This is slightly lower than the productivity of PLAL of CuO powder, but still relatively high compared to the ablation of bulk targets with the same laser set-up. In a first approximation, the amount of generated particles correlates linearly to the number of laser pulses as depicted by the solid line in Fig. 4d. While the PLFL is remarkably reproducible in terms of the particle size distribution, the quantitative reproducibility between similar samples is quite limited. This is a well known flaw of the batch approach used here and will significantly improve as free jets are used to perform PLFL.²³ It can be stated that PLFL of CuI powder makes it feasible to produce about 5 mg CuI nanoparticles per hour with the given set-up.

4 Conclusion

It has been shown that the irradiation of a suspended μm-sized CuI powder with a pulsed laser leads to the formation of a stable CuI colloid. The CuI nanoparticles show a log-normal size distribution with a mean diameter of 31 nm in water and 18 nm in ethyl acetate. Further laser irradiation increases the number of generated nanoparticles, while there is only a minor effect on the size distribution, leading to the conclusion that the final size is characteristic for this material. The chemical composition and crystal structure of generated nanoparticles can be unambiguously assigned to pure CuI. The synthesis of stable CuI colloids by pulsed laser fragmentation in liquids, marks an extension of the existing synthesis possibilities of laser assisted nanoparticle generation. While several other precursor powders follow a reductive ablation and nucleation mechanism, CuI is a textbook example for a fragmentation mechanism.

5 Acknowledgement

The authors would like to thank Yeliz Akyürek and Michael W. Linscheid (Humboldt-Universität zu Berlin) for the flame atomic absorption spectrometry measurements and C. Schmidt and K.-H. Lerche (microParticles GmbH) for the analytical disc centrifuge measurements.

References

- 1 D. B. Geohegan, A. A. Poretzky, G. Duscher, S. J. Pennycook, *Appl. Phys. Lett.*, 1998, **72**, 2987–2989.
- 2 A. Henglein, *J. Phys. Chem. B*, 1993, **97**, 5457–5471.
- 3 A. Solliera, L. Berthe, R. Fabbro, *Eur. Phys. J. Appl. Phys.*, 2001, **16**, 131–139.
- 4 G. W. Yang, *Prog. Mater. Sci.*, 2007, **52**, 648–698.
- 5 J. S. Golightly, A. W. Castleman, *J. Phys. Chem. B*, 2006, **110**, 19979–19984.
- 6 K. Y. Niu, J. Yang, S. A. Kulinich, J. Sun, H. Li, X. W. Du, *J. Am. Chem. Soc.*, 2010, **132**, 9814–9819.
- 7 B. Brandt, J.-H. Fischer, W. Ludwig, J. Libuda, F. Zaera, S. Schauerermann, H.-J. Freund, *J. Phys. Chem. C*, 2008, **112**, 11408–11420.
- 8 A. V. Simakin, G. A. Shafeev, E. N. Loubnin, *Appl. Surf. Sci.*, 2000, **154–155**, 405–410.
- 9 J. Turkevich, P. C. Stevenson, J. Hillier, *Discuss. Faraday Soc.*, 1951, **11**, 55–75.
- 10 P. V. Kazakevich, A. V. Simakin, V. V. Voronov, G. A. Shafeev, *Appl. Surf. Sci.*, 2006, **252**, 4373–4380.
- 11 S. Barcikowski, G. Compagnini, *Phys. Chem. Chem. Phys.*, 2013, **15**, 3022–3026.
- 12 M.-S. Yeh, Y.-S. Yang, Y.-P. Lee, H.-F. Lee, Y.-H. Yeh, C.-S. Yeh, *J. Phys. Chem. B*, 1999, **103**, 6851–6857.
- 13 C. A. Schaumberg, M. Wollgarten, K. Rademann, *J. Phys. Chem. A*, 2014, **118**, 8329–8337.
- 14 I. Tanaka, M. Nakayama, *J. Appl. Phys.*, 2002, **92**, 3511–3516.
- 15 A. Klapars, S. L. Buchwald, *J. Am. Chem. Soc.*, 2002, **124**, 14844–14845.
- 16 R. Shimizu, H. Egami, Y. Hamashima, M. Sodeoka, *Angew. Chem. Int. Ed.*, 2012, **51**, 4577–4580.
- 17 T. Heil, H. Kohl, *Ultramicroscopy*, 2010, **110**, 748–753.

-
- 18 S. Hull, D. A. Keen, *Phys. Rev. B*, 1994, **50**, 5868–5885.
- 19 R. F. Egerton, *Electron Energy-Loss Spectroscopy in the Electron Microscope*, 3rd ed., Springer, New York, Dordrecht, Heidelberg, London, 2011, pp. 424–425.
- 20 L. V. Zhigilei, B. J. Garrison, *Appl. Surf. Sci.*, 1998, **127-129**, 142–150.
- 21 H. Cai, N. Chaudhary, J. Lee, M. F. Becker, J. R. Brock, J. W. Keto, *J. Aerosol Sci.*, 1998, **29**, 627–636.
- 22 T. T. P. Nguyen, R. Tanabe, Y. Ito, *Appl. Phys. Lett.*, 2013, **102**, 124103.
- 23 M. Lau, S. Barcikowski, *Appl. Surf. Sci.*, 2014, <http://dx.doi.org/10.1016/j.apsusc.2014.07.053>.